Pergamon

Int. J. Heat Mass Transfer. Vol. 40, No. 4, pp. 785–798, 1997

0017-9310/97 $17.00+0.00

PII: S0017-9310(96)00161-5

Rayleigh–Marangoni thermoconvective instability with non-Boussinesq corrections

R. SELAK and G. LEBON†

Liège University, Institute of Physics B5, Sart Tilman, B-4000 Liège, Belgium

(*Received* 10 *May* 1995 *and in final form* 8 *May* 1996)

Abstract—A linear analysis of coupled surface tension and gravity driven instabilities in fluids with variable thermophysical properties is proposed. The fluid layer is initially at rest, of infinite horizontal extent, limited by two flat boundaries and subject to a vertical temperature gradient. Viscosity is supposed to vary exponentially with respect to the temperature, while linear laws are assumed for the heat capacity and thermal conductivity. The relative departure from the Boussinesq model, where fluid properties are constant, is derived by selecting reference properties at the bottom temperature. A physical interpretation of non-Boussinesq effects on the critical threshold is proposed. Computations for glycerol and liquid potassium show that the temperature dependence of the thermophysical properties may have a significant influence on the onset of convection. Copyright © 1996 Elsevier Science Ltd.

1. INTRODUCTION

The problem of thermal convection in a horizontal fluid layer is usually based on the Boussinesq approximation [1–4] stating, in particular, that the temperature dependence of the fluid properties is negligible except for density differences involved in the buoyancy force. Except for some fluids, thermal conductivity, heat capacity and viscosity may also vary with temperature so that Boussinesq's approximation becomes questionable [5]. In the present work, we examine to what extent the temperature dependence of the three thermophysical coefficients can alter the onset of convection in the coupled Rayleigh–Marangoni instability [6]. In such a problem, two motors of instability are present [4, 6]: the first results from the thermal expansion responsible for the buoyancy effect (Rayleigh–Bénard problem), the second is the variation of surface tension with temperature (Marangoni problem). In the present work, we limit ourselves to a linear analysis.

For most fluids, viscosity is more sensitive to temperature variations than heat capacity and thermal conductivity. Liquids can undergo strong viscosity variations which are usually well described by exponential laws [7–9]. On the other hand, heat capacity and thermal conductivity for gases and liquids are well represented by linear functions of the temperature [10, 11]. When the thermal conductivity depends linearly on temperature, the temperature profile in the conductive reference state is no longer linear. It follows that the equations describing the velocity and temperature perturbations will contain additional terms with respect to Boussinesq's approximation. Convection in fluids whose material coefficients are temperature-dependent are of interest in geophysical problems as well as in engineering applications such as solidifications of thin coats and crystallization processes.

The mathematical model that accounts for the non-Boussinesq contributions is given in Section 2. The critical temperature difference across the layer is calculated in Section 3 by means of the normal mode technique. In Section 4, it is shown that by appropriately selecting the reference viscosity and heat diffusivity, one obtains a direct estimation of the relative error on the critical temperature difference with respect to the Boussinesq model. A physical interpretation of the results is also proposed. Combined non-Boussinesq effects are investigated in Section 5. The general analysis is applied to the particular case of a glycerol layer and a liquid potassium layer for which at least two physical parameters vary strongly with temperature.

2. THE BASIC EQUATIONS AND BOUNDARY CONDITIONS

We consider a thin layer of an incompressible Newtonian fluid with thickness d and infinite horizontal extent. A cartesian reference frame with its origin at the bottom of the layer and its axis $\mathbf{e}_3$ pointing vertically in the opposite direction of gravity is selected. The lower boundary is uniformly heated at tempera-

† Author to whom correspondence should be addressed. Also at Louvain University, Department of Mechanics, B-1348 Louvain-la-Neuve, Belgium.

NOMENCLATURE

- a parameter defined in equation (18)
- A non-dimensional thermal conductivity parameter
- A_1, A_2, B coefficients defined in equations (10) and (11)
- c, c^* kinematic and dynamical viscosity contrasts
- c_p heat capacity
- C non-dimensional heat capacity parameter
- d fluid layer depth
- $\mathbf{e}_3$ vertical unit vector
- f, f^* non-dimensional kinematic and dynamical viscosities in the basic state
- g gravitational acceleration
- h Biot number $\equiv Hd/K_0$
- $\tilde{h}$ generalized Biot number
- H heat transfer coefficient
- k wave number $\equiv \|\mathbf{k}\|$
- $\mathbf{k}$ horizontal wave number vector $(k_1, k_2, 0)$
- k_0 reference thermal diffusivity
- K thermal conductivity
- L non-dimensional viscosity parameter
- $\mathbf{M}$ square matrix of dimension six by six
- Ma Marangoni number $\equiv (-\partial\xi/\partial T)\,\Delta T d/\mu_0 k_0$
- P pressure
- Pr Prandtl number $\equiv \mu_0/\rho_0 k_0$
- r_a, r_c, r_e non-Boussinesq parameters associated with variable thermal conductivity, heat capacity and viscosity, respectively
- Ra Rayleigh number $\equiv \rho_0 g \alpha_0 \Delta T a^3/\mu_0 k_0$
- s growth rate with time
- t time
- T temperature
- T_∞ mean temperature of the outer medium
- u_1, u_2, u_3 velocity field
- V_1, V_2, V_3 perturbation velocity field
- W amplitude of perturbation vertical velocity
- x_1, x_2, x_3 cartesian co-ordinates
- X non-dimensional co-ordinates (X_1, X_2, X_3)
- $\mathbf{Y}$, $\mathbf{Y}_n$, $\mathbf{Z}_n$ vectors of dimension six.

Greek symbols

- α coefficient of thermal expansion
- α_n arbitrary coefficients
- γ, κ, χ fluid property coefficients
- δ Euclidian norm of the vector (Ra, Ma)
- δ_{ij} Kronecker delta symbol
- Δ relative variation of δ
- ΔT difference between the boundary temperatures $\equiv T_0 - T_1$
- ε_1, ε_2 non-dimensional parameters defined in equation (5)
- ϑ non-dimensional perturbation temperature
- θ, θ_N angles in degrees
- Θ amplitude of perturbation temperature
- μ dynamical viscosity
- ν kinematic viscosity
- ξ surface tension
- Π non-dimensional perturbation pressure
- ρ density
- σ real part of the growth rate s
- τ non-dimensional time
- ψ, Ψ field variables
- ω imaginary part of the growth rate s.

Subscripts

- 0 refers to conditions at the rigid boundary temperature
- 1 refers to conditions at the free boundary temperature
- B refers to conditions in the Boussinesq approximation
- i,j integers from 1 to 3
- m refers to conditions at the mean temperature $T_m = (T_0 + T_1)/2$
- n integer from 1 to 6
- ref reference steady conductive state.

Superscripts

- c critical conditions
- $(\,)'$ disturbance of the associated variable.

ture T_0, while the upper undeformable surface is held at a cooler temperature T_1. The relevant thermohydrodynamic equations are:

$$\frac{\partial u_i}{\partial x_i} = 0 \tag{1}$$

$$\rho_0 \frac{du_i}{dt} = -\rho_0[1-\alpha_0(T-T_0)]g\delta_{i3} - \frac{\partial P}{\partial x_i} + \frac{\partial}{\partial x_j}\left[\mu\left(\frac{\partial u_i}{\partial x_j} + \frac{\partial u_j}{\partial x_i}\right)\right] \tag{2}$$

$$\rho_0 c_p \frac{dT}{dt} = \frac{\partial}{\partial x_j}\left[K\frac{\partial T}{\partial x_j}\right] \quad (i,j = 1,2,3). \tag{3}$$

We have used the summation convention on repeated indices. Notation u_i is used for the components of the fluid velocity, P for pressure and T for temperature, μ is the dynamical viscosity, c_p the heat capacity, K the thermal conductivity and g the acceleration due to gravity. Quantities with subscript 0 are constants evaluated at some arbitrary reference temperature which for definiteness is chosen as the bottom boundary temperature T_0. The operator $d/dt = (\partial/\partial t) + u_i(\partial/\partial x_i)$ stands for the material time derivative. In the above equations, the thermophysical properties of the fluid c_p, K and μ are temperature-dependent and the density ρ is given by the state equation

$$\rho(T) = \rho_0[1 - \alpha_0(T - T_0)] \tag{4}$$

where α_0 is the coefficient of thermal expansion.

According to Mihaljan [2], equations (1)–(3) may be viewed as a first order approximation to the Navier–Stokes equations when all the state variables P, T, u_i are expanded in a power series of two independent non-dimensional parameters

$$\varepsilon_1 = \alpha_0 \Delta T \quad \varepsilon_2 = \frac{k_0^2}{c_{p0} d^2 \Delta T} \tag{5}$$

where c_{p0} and k_0 denote a reference heat capacity and thermal diffusivity, respectively. The quantity $\Delta T = T_0 - T_1$ is the temperature difference between the lower and upper boundaries. It must be stressed that equations (1)–(3) share some of the assumptions included in the Boussinesq approximation, namely:

- density is constant everywhere, except in the gravity term of equation (2);
- viscous dissipation and energy fluctuations with pressure are neglected in the energy balance of equation (3).

The important departure from the Boussinesq simplification is that thermophysical coefficients are not required to be constant *a priori*. The set of equations (1)–(3) is rigorously justified under the conditions

$$\varepsilon_1 \ll 1 \quad \varepsilon_2 \ll 1 \tag{6}$$

which are generally met for thermoconvective flows in thin fluid layers.

In the reference state, the fluid layer is at rest ($u_i^{\text{ref}} = 0$) and heat propagates by conduction only. When the thermal conductivity is a constant, the reference temperature field is simply

$$T_{\text{ref}}(x_3) = T_0 - \Delta T x_3/d. \tag{7}$$

Now, if the thermal conductivity varies with temperature according to the linear law

$$K(T) = K_0[1 - \kappa_0(T - T_0)] \tag{8}$$

the reference temperature profile is no longer given by equation (7) but, in dimensionless form, by

$$\vartheta_{\text{ref}} \equiv \frac{T_{\text{ref}} - T_0}{\Delta T} = \frac{1}{A}[1 - (1 + BX_3)^{1/2}] \tag{9}$$

with

$$A = \kappa_0 \Delta T \quad B = 2A(1 + A/2) \quad X_3 = x_3/d. \tag{10}$$

Although expression (9) is singular for A = 0, it has a well-defined limit for A tending to zero. Indeed, a regular temperature profile can be derived from equation (9) by means of a power series in terms of BX_3; up to the second order in X_3 one has:

$$\vartheta_{\text{ref}} = A_1 X_3 + A_2 X_3^2 \tag{11}$$

where the coefficients A_1 and A_2 are expressed by

$$A_1 = -\left(1 + \frac{A}{2}\right) \quad A_2 = \frac{A}{2}\left(1 + \frac{A}{2}\right)^2. \tag{12}$$

Expansion (11) is valid under the condition $|BX_3| < 1$ which is satisfied for

$$-1 - \sqrt{2} < A < -1 + \sqrt{2}. \tag{13}$$

In addition, the positiveness of the thermal conductivity, equation (8), requires that $A > -1$ from which it follows that the profile of equation (11) is valid for values of A restricted to the interval

$$-1 < A < -1 + \sqrt{2}. \tag{14}$$

The heat flux across the interface is modeled by Newton's cooling law

$$-K\frac{\partial T}{\partial x_3} = H(T - T_\infty) \tag{15}$$

where $H(\geqslant 0)$ is the heat transfer coefficient at the interface and T_∞ is the constant mean temperature of the external medium. Assuming a constant thermal conductivity and introducing the reference conductive state of equation (7) into equation (15), it was found by Pearson [12] that the temperature difference across the layer is

$$\Delta T = \frac{h(T_0 - T_\infty)}{(1 + h)} \tag{16}$$

where $h = Hd/K_0$ is the Biot number. However, for a variable thermal conductivity, equation (16) becomes more complex and it is found that

$$\Delta T = \frac{-(1 + h) + \sqrt{(1 + h)^2 + 2ah}}{a}(T_0 - T_\infty) \tag{17}$$

with

$$a = \kappa_0(T_0 - T_\infty). \tag{18}$$

Expression (17) is interesting as it provides an indirect way to determine the Biot number by measuring ΔT.

The heat capacity of a fluid may also change with temperature; albeit small, its variation is generally of the same order of magnitude as that of thermal conductivity and it is usual to represent the dependence of c_p with respect to T by a linear law

$$c_p(T) = c_{p0}[1-\chi_0(T-T_0)]. \tag{19}$$

For further calculations one introduces the non-dimensional number

$$C = \chi_0 \Delta T. \tag{20}$$

Inspection of equations (8) and (19) shows that A and C express the relative variations of K and c_p with respect to the temperature; in the same way as A, the quantity C is strictly greater than -1.

The dynamical viscosity $\mu(T)$ in liquids is generally more sensitive to temperature variations than the heat capacity or the thermal conductivity and is therefore represented by an exponential law

$$\mu(T) = \mu_0 \exp[-\gamma_0(T-T_0)] \quad \gamma_0 \geqslant 0. \tag{21}$$

By analogy with A and C given by equations (10) and (20), let us define L by the non-dimensional quantity

$$L = \gamma_0 \Delta T. \tag{22}$$

It is widely admitted [7, 9] that the law of equation (21) fits fairly well for strong viscosity variations in liquids such as silicone oils or glycerol.

Although the parameters ε_1 and ε_2 are required to remain small, the parameters A, C, L may be varied to any size as they are expressed in terms of κ_0, χ_0, γ_0, respectively, which are not necessarily small. Instead of quantifying the dependence of K, c_p, μ with respect to the temperature by means of the three so-called non-Boussinesq parameters A, C, L, it is equivalent to use the three quantities

$$r_a = 1+A \quad r_c = 1+C \quad r_e = \exp(L) \tag{23}$$

each of them being equal to the ratio of the corresponding thermophysical coefficient at temperature T_1 to its value at temperature T_0. The Boussinesq approximation corresponds then to $A = C = L = 0$ (or equivalently $r_a = r_c = r_e = 1$).

We now formulate the evolution equations for the infinitesimally small disturbances T', P', u_i'. After using the following scaling for the space co-ordinates, time, velocity, pressure, and temperature,

$$X_i = \frac{x_i}{d} \quad \tau = t\frac{k_0}{d^2} \quad V_i = u_i'\frac{d}{k_0} \quad \Pi = P'\frac{d^2}{k_0^2} \quad \vartheta = \frac{T'}{\Delta T} \tag{24}$$

respectively, with $k_0 = K_0/\rho_0 c_0$ a reference thermal diffusivity, the linearized dimensionless equations can be written as:

$$\frac{\partial V_i}{\partial X_i} = 0 \tag{25}$$

$$Pr^{-1}\left(\frac{dV_i}{d\tau} + \frac{\partial \Pi}{\partial X_i}\right) = Ra\vartheta\,\delta_{i3} + \frac{\partial}{\partial X_j}\left[\tilde{\mu}\left(\frac{\partial V_i}{\partial X_j} + \frac{\partial V_j}{\partial X_i}\right)\right] \tag{26}$$

$$\tilde{c}\left(\frac{d\vartheta}{d\tau} + D\vartheta_{ref}V_3\right) = \frac{\partial}{\partial X_j}\left(\tilde{K}\frac{\partial \vartheta}{\partial X_j} - AD\vartheta_{ref}\vartheta\,\delta_{j3}\right) \tag{27}$$

where D stands for $\partial/\partial X_3$. The remaining undefined quantities in equations (26) and (27) are $\tilde{K} = 1 - A\vartheta_{ref}$, $\tilde{c} = 1 - C\vartheta_{ref}$, $\tilde{\mu} = \exp(-L\vartheta_{ref})$, while Pr and Ra are the Prandtl and Rayleigh numbers:

$$Pr = \frac{\mu_0}{\rho_0 k_0} \quad Ra = \frac{\rho_0 g \alpha_0 \Delta T d^3}{k_0 \mu_0}. \tag{28}$$

The lower boundary is supposed to be flat, rigid and perfectly heat conducting so that its temperature remains constant at T_0, therefore, it follows that

$$V_3 = \vartheta = 0 \quad \text{at } X_3 = 0. \tag{29}$$

The upper boundary of the fluid is assumed to be free, undeformable but submitted to a surface tension ξ depending linearly on the temperature:

$$\xi(T) = \xi(T_0) + \frac{\partial \xi}{\partial T}(T-T_0). \tag{30}$$

Assuming that the external environment is inert and quiescent, the corresponding boundary conditions at the upper surface are

$$V_3 = 0 \quad -Ma\frac{\partial \vartheta}{\partial X_i} = \tilde{\mu} DV_i \quad (i = 1,2) \quad \text{at } X_3 = 1 \tag{31}$$

where the Marangoni number Ma is defined by

$$Ma = \frac{(-\partial \xi/\partial T)\Delta T d}{\mu_0 k_0}. \tag{32}$$

Although condition (31) is written at $X_3 = 1$, the reference viscosity μ_0 and diffusivity k_0 entering into the definition of Ma are taken at the bottom temperature T_0. It will be shown in Section 4 that this definition of Ma allows for a clearer and easier physical interpretation of the numerical results.

After perturbing the reference state and linearizing equation (15), one obtains the dimensionless expression

$$\tilde{h}\vartheta + D\vartheta = 0 \quad \text{at } X_3 = 1 \tag{33}$$

where $\tilde{h}$ stands for

$$\tilde{h} = \frac{h - A[D\vartheta_{ref}]_{X_3=1}}{1 - A[\vartheta_{ref}]_{X_3=1}}. \tag{34}$$

Equation (33) is formally identical to the classical relation $h\vartheta + D\vartheta = 0$ obtained [12] for a constant thermal conductivity. By extension, $\tilde{h}$ will be called the generalized Biot number; it is a function of h and A with $\tilde{h} = h$ for $A = 0$. Starting from the exact reference profile of equation (9), it is found that the difference between $\tilde{h}$ and h is

$$\tilde{h} - h = A\left[\frac{(1+A/2)}{(1+A)} - h\right]. \tag{35}$$

The quantity $\tilde{h}$ is not only equal to h for $A = 0$, but also for a particular value of the Biot number given by $h^* = (1+A/2)/(1+A)$. For positive values of A and

$h < h^*$ one has $\tilde{h} > h$, while for $h > h^*$ one has $\tilde{h} < h$. For negative values of A and $h < h^*$, it is checked that $\tilde{h} < h$ and for $h > h^*$, it is found that $\tilde{h} > h$. Consequently, when A is negative and the interface adiabatically insulated ($h = 0$), the generalized Biot number may become negative. This situation would correspond to a reversed heat flow across the interface towards the interior of the layer; instability is then reinforced compared to the case of a constant thermal conductivity.

3. NORMAL MODE ANALYSIS

According to the normal mode technique, we seek solutions of equations (25)–(27) of the form

$$\Psi(X_1, X_2, X_3, \tau) = Re\{\psi(X_3)\exp[i(\mathbf{k}\cdot\mathbf{X}) + s\tau]\} \tag{36}$$

where $\mathbf{k}$ is the horizontal wave number of the disturbance with $\mathbf{k} = (k_1, k_2, 0)$, $k = \|\mathbf{k}\|$, $X = (X_1, X_2, X_3)$ and $s = \sigma + i\omega$. States of marginal or neutral stability are characterized by a zero growth rate σ; if in addition $\omega = 0$, one speaks about exchange of stability, while, for $\omega \neq 0$, corresponding to oscillatory convective motions, the situation is referred to as overstable.

After introducing expression (36) into equations (25)–(27), (29), (31), (33) and eliminating the horizontal components of velocity, one obtains the two following ordinary differential equations:

$$Pr^{-1}s(D^2 - k^2)W = -k^2 Ra\Theta + \tilde{\mu}(D^2 - k^2)^2 W + 2(D\tilde{\mu})(D^2 - k^2)DW + (D^2\tilde{\mu})(D^2 + k^2)W \tag{37}$$

$$\tilde{c}(s\Theta + D\vartheta_{ref}W) = \tilde{K}(D^2 - k^2)\Theta + 2(D\tilde{K})D\Theta + (D^2\tilde{K})\Theta \tag{38}$$

where $W(X_3)$ and $\Theta(X_3)$ are the amplitude of the vertical component of the velocity and the temperature disturbances, respectively. The six corresponding boundary conditions are:

$$W = 0 \quad DW = 0 \quad \Theta = 0 \quad \text{at } X_3 = 0 \tag{39}$$

$$W = 0 \quad \tilde{h}\Theta + D\Theta = 0$$

$$k^2 Ma\Theta + \tilde{\mu}D^2 W = 0 \quad \text{at } X_3 = 1. \tag{40}$$

Observe that only the norm of the wave number $\mathbf{k}$ enters into the problem which means that no particular horizontal direction is privileged. It is also well known [13] that a linear analysis does not allow one to determine which kind of cellular pattern will arise at the onset of convection.

The eigenvalue problem set up by equations (37) and (38) is solved by the shooting method (e.g. as in ref. [14]) and requires in principle the six boundary conditions of equations (39) and (40). However, as shown below, it is possible to proceed by using only three conditions. For clarity, equations (37) and (38) can be written in the form

$$D\mathbf{Y} = \mathbf{M}\mathbf{Y} \tag{41}$$

where $\mathbf{Y}$ stands for the vector $[W, DW, D^2W, D^3W, \Theta, D\Theta]^\perp$ and $\mathbf{M}$ for a six by six square matrix function whose entries are X_3-dependent. Any solution of equation (41) can be expressed [15] in the form

$$\mathbf{Y} = \sum_{n=1}^{6} \alpha_n \mathbf{Y}_n \tag{42}$$

where $\mathbf{Y}_n (n = 1, \ldots, 6)$ are six-dimensional vectors, which will be shown to form a fundamental basis. First, we reduce the boundary value problem to an initial value problem by imposing arbitrary values to each solution $\mathbf{Y}_n$ at one end point of the domain $X_3 \in [0, 1]$. Let $\mathbf{Z}_n$ denote the nth unit vector of dimension six whose components are all zero except the nth which is equal to one. Taking $\mathbf{Y}_n$ equal to $\mathbf{Z}_n$ at $X_3 = 0$, one is allowed to build the various solutions by numerically integrating the differential system, equation (41), with a Runge–Kutta scheme from $X_3 = 0$ to the endpoint $X_3 = 1$. It is proved [16] that the set of obtained solutions $\mathbf{Y}_n$ is linearly independent over the domain [0, 1] and that their linear combination, equation (42), is the general solution of equation (41). With such a basis, let us calculate the value of the coefficients α_n.

The three boundary conditions of equation (39) are satisfied if and only if $\alpha_1 = \alpha_2 = \alpha_5 = 0$. The linear combination of equation (42) is afterwards introduced into the conditions of equation (40); this procedure results in three linear homogeneous equations in the unknown coefficients of $\mathbf{Y}_3$, $\mathbf{Y}_4$ and $\mathbf{Y}_6$. This homogeneous algebraic system is solvable if and only if its determinant is equal to zero. This yields an expression of the Marangoni number in terms of the remaining parameters $\{\omega, Pr, Ra, k, h, A, C, L\}$. Since the Marangoni number is a real physical quantity, the occurrence of an oscillatory state is subordinated to the search of an ω-value for which the imaginary part of Ma vanishes.

We have investigated the following range of parameters:

$$0 \leqslant Pr^{-1} \leqslant 100 \quad -2000 \leqslant Ra \leqslant 2000 \quad 0 \leqslant k \leqslant 10$$

$$0 \leqslant h \leqslant 1000 \quad -0.28 \leqslant A \leqslant 0.4$$

$$-0.28 \leqslant C \leqslant 0.4 \quad -2.3 \leqslant L \leqslant 2.3$$

and found that $\omega = 0$ is the single value corresponding to $\mathrm{Im}[Ma] = 0$. Absence of overstability has already been shown numerically in the particular case of constant thermophysical coefficients for the pure Marangoni problem [17] and for the surface tension and buoyancy-driven convective instability [18]. The range of variation of the parameters Pr, Ra, k and h is close to those found in the works by Vidal and Acrivos [17] and Takashima [18]. Concerning the parameters A and C, experimental data are rather scarce. In Tables

Table 1. Thermophysical data for several liquids used in convective instability experiments

Liquid (T_0 in °C)	γ_0	κ_0	χ_0	Pr	References
Mercury (25)	0.0039	−0.0028	0.0002	0.024	[19]
Water (25)	0.022	−0.0026	0.0001	6.2	[20, 21]
Aroclor 1248 (40)	0.091	0	0	650	[21]
Silicone oil 47V100 (25)	0.023	0	0	880	[22]
Silicone oil 47V1000 (25)	0.02	0	0	9720	[23]
Polybutene oil no. 8 (25)	0.085	0.0015	−0.0027	43000	[24]
Polybutene oil L100 (20)	0.09	−0.001	−0.0003	13000	[24, 25]
Golden syrup (25)	0.16	−0.005	0	158000	[23, 25, 26]

1 and 2, the values of γ_0, κ_0 and χ_0 (in K^{-1} unit) for various liquids are compiled [7, 9–11, 19–27]. Assuming a typical critical temperature drop $\Delta T^c = 10$K, it is seen that 0.4 provides a reasonable upper bound for A and C; the corresponding value of the associated ratio is 1.4 and its reciprocal is 0.71 leading to a lower bound of −0.28. We note also from the data of Tables 1 and 2 that the heat capacity and the thermal conductivity may indifferently decrease or increase with the temperature. On the other hand, experiments indicate [28] that the rate of viscosity change is much larger than for heat capacity and conductivity. This justifies the wide range of variation of L.

Since within the range of parameters examined above, exchange of stability is satisfied, we shall from now on assume that the marginal state is steady with $\sigma = s = 0$. The eigenvalue problem is therefore governed by the dimensionless numbers $\{Ra, Ma, k, h, A, C, L\}$; by fixing Ra, h, A, C, L, it is possible to represent Ma as a function of the wave number k. In all cases, the marginal stability curve is a unimodal function and presents a single minimum, say Ma^c, at which the motionless layer becomes unstable with respect to infinitesimal perturbations.

4. DISCUSSION

In Figs. 1–3 are plotted the values of Ma^c vs Ra^c when the viscosity, thermal conductivity and heat capacity are varied separately. The co-ordinates of these three graphs are restrained to positive values ($Ra^c > 0$ and $Ma^c > 0$), which correspond either to the case of a fluid layer heated from below with $\alpha_0 > 0$ or to a fluid adhering to a hot ceiling with $\alpha_0 < 0$. For the moment, the Biot number is fixed at a value equal to zero. Each curve divides the plane Ra^c–Ma^c in two

Table 2. Thermophysical data for glycerol and liquid potassium

	Glycerol (25°C)	Potassium (700°C)
ρ_0 [kg m^{-3}]	1258.4	681.5
α_0 [10^{-4} K^{-1}]	4.9	3.3
μ_0 [10^{-4} kg m^{-1} s^{-1}]	927.4	2.5
γ_0 [10^{-3} K^{-1}]	93.4	0.8
K_0 [W m^{-1} K^{-1}]	0.284	32.52
κ_0 [10^{-3} K^{-1}]	0.487	0.723
C_{p0} [J kg^{-1} K^{-1}]	2418	773.5
χ_0 [10^{-4} K^{-1}]	−25.97	−0.84
k_0 [10^{-6} m^2 s^{-1}]	0.093	61.7
$-\partial\xi/\partial T$ [10^{-4} N m^{-1} K^{-1}]	1.3	0.625
Pr	790	0.006

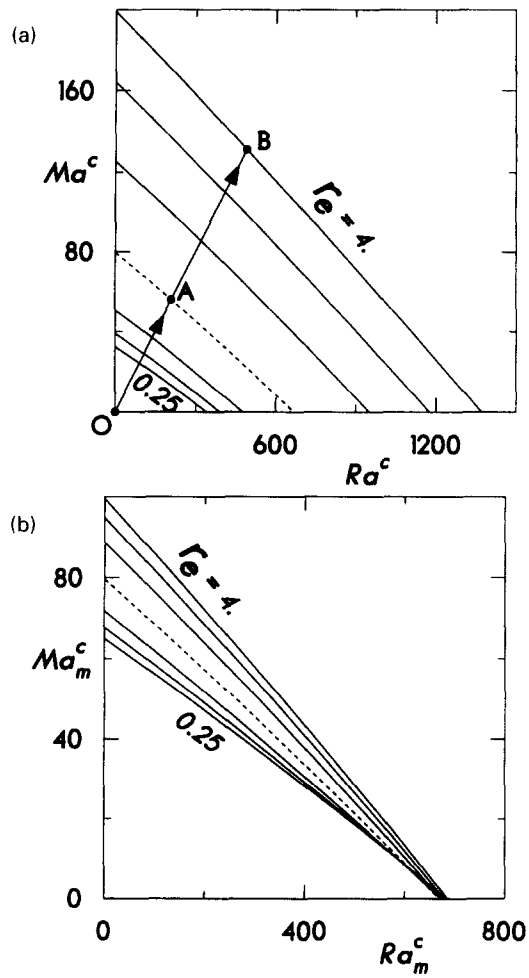

Fig. 1. Critical Marangoni number versus the critical Rayleigh number for several values of $r_e (r_a = r_c = 1, h = 0)$. The different r_e values are 4, 3, 2, 1, 1/2, 1/3, 1/4, by going down from the highest to the lowest curve. The dashed curve refers to Boussinesq's approximation. (a) Ra^c and Ma^c are defined by using the temperature of the bottom plate as reference. (b) Ra^c_m and Ma^c_m are defined with the mean temperature T_m.

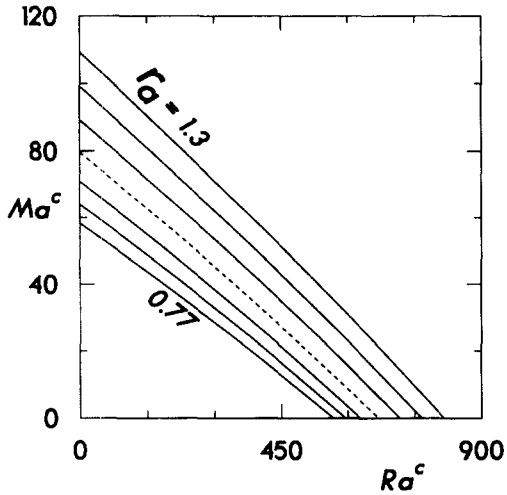

Fig. 2. Influence of a variable thermal conductivity ($r_c = r_e = 1, h = 0$) on the instability threshold. The co-ordinates are the same as in Fig. 1(a). The values of r_a are, from the highest to the lowest curve: 1.3, 1.2, 1.1, 1, 1/1.1, 1/1.2, 1/1.3.

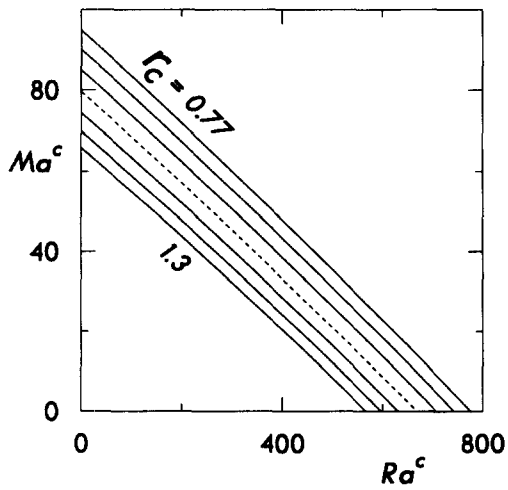

Fig. 3. Influence of a variable heat capacity ($r_a = r_e = 1$, $h = 0$) on the instability threshold. The co-ordinates are the same as in Fig. 1(a). The values of r_c are, from the highest to the lowest curve: 1/1.3, 1/1.2, 1/1.1, 1, 1.1, 1.2, 1.3.

areas; the representative points found below the curve describe stable situations, while the points above the curve refer to unstable states. Each curve determines an instability threshold formed by the locus of points (Ra^c, Ma^c) for fixed h, A, C, L values. In each figure, the dashed line corresponds to a fluid whose physical properties are constant and will be taken as a reference in order to show the deviations of the results with respect to Boussinesq's approximation. The critical points take the form of a beam of curved lines moving continuously as the selected parameter r_a, r_c or r_e is altered. The graphs in Figs. 1–3 illustrate the influence of the non-Boussinesq effects upon the critical temperature difference ΔT^c. In fact, eliminating ΔT between Ra and Ma yields the equation of a straight line

$$Ma = \frac{-\partial\xi/\partial T}{\rho_0\alpha_0 g d^2} Ra. \tag{43}$$

This means that, for a layer of fixed depth d whose thermophysical properties are known, the slope of the straight line, equation (43), is prescribed and, when ΔT grows, one moves along the straight line OAB. The critical ΔT^c is determined by the crossing point between the straight line of equation (43) and a given instability curve (point A or B in Fig. 1(a)). Only the dashed curve, corresponding to Boussinesq's approximation, remains fixed in the plane Ra^c–Ma^c when ΔT is varied. In contrast, the solid curves corresponding to non-Boussinesq fluids will move in the plane Ra^c–Ma^c when ΔT is changed, since A, C, L are themselves proportional to ΔT. The length of the segment joining the origin O of the plane Ra^c–Ma^c to an intersection point is equal to

$$\delta = \sqrt{(Ra^c)^2 + (Ma^c)^2} = \frac{d\sqrt{(\partial\xi/\partial T)^2 + (\rho_0\alpha_0 g d^2)^2}}{\mu_0 k_0} |\Delta T^c|. \tag{44}$$

An original aspect of the present work is the use of a reference viscosity taken at the bottom temperature T_0 in the definition of the Rayleigh and Marangoni numbers instead of the mean temperature between the lower and upper boundaries as used by many authors. This choice is motivated firstly by the fact that in the present problem the symmetry with respect to the mid-plane is lost and secondly by the requirement to establish a strict proportionality between δ and ΔT^c, allowing for a more convenient physical interpretation of the results. Consequently, since δ does not depend on A, C, L, the relative variation Δ $(= \delta - \delta_B/\delta_B)$ is exactly equal to the relative variation of the critical temperature threshold between the non-Boussinesq and Boussinesq theories; indeed, one has

$$\Delta = \frac{\delta - \delta_B}{\delta_B} = \frac{\Delta T^c - \Delta T_B^c}{\Delta T_B^c} \tag{45}$$

where δ_B is the value of δ in the Boussinesq approximation.

We have checked the validity of our results by comparison with those of Stengel *et al.* [7] who studied the pure Rayleigh problem in the case of a viscosity varying exponentially with temperature. However, before performing this comparison, a remark must be set in form. The balance equation (1) (p. 413 of Stengel *et al.* [7]) contains the quantity

$$f = \nu(T_{ref})/\nu(T_m) \tag{46}$$

where ν is the kinematic viscosity and $T_m = (T_0 + T_1)/2$ is the mean value of the boundary temperature. To be correct, this expression should be replaced by

$$f^* = \mu(T_{ref})/\mu(T_m) \tag{47}$$

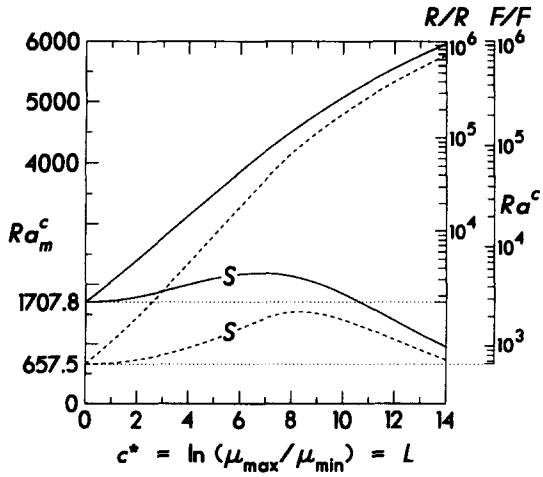

Fig. 4. Critical Rayleigh number vs the variable viscosity parameter L for the Rayleigh–Bénard problem with rigid–rigid (R–R, solid lines) or free–free (F–F, dashed lines) perfectly heat conducting boundaries. The left ordinate scale is linear and the right one is logarithmic. By taking T_m as the reference temperature, one recovers Stengel's curves (denoted by label S); with T_0 as reference temperature, the curves exhibit a monotonous increase.

where μ denotes the dynamical viscosity. This is easily checked by starting from our equation (2) where all the constants are taken at the mean temperature T_m and by using the scalings adopted by Stengel *et al.* [7]. A similar conclusion can be reached from the work of Busse and Frick [29]. Although the non-dimensional variables used by Busse and Frick [29] are different from those of Stengel *et al.* [7], it is nevertheless the ratio of equation (47) which emerges in the diffusion term (see equation (2.2.a), p. 453 in ref. [29]). As a consequence, the viscosity contrast $c = \ln(\nu_{max}/\nu_{min})$ defined by Stengel *et al.* [7] (equation (10), p. 414) should be replaced by

$$c^* = \ln(\mu_{max}/\mu_{min}) = L \tag{48}$$

where L is the quantity defined in the present work through equation (22).

It must be stressed that by taking a different reference temperature and hence a different reference viscosity, the behaviour of the critical Rayleigh number with respect to the parameter L may be drastically modified. This peculiarity was pointed out by several authors, such as Bottaro *et al.* [30] for the pure Rayleigh problem, Selak and Lebon [31] for Rayleigh–Marangoni instability and Slavtchev and Ouzounov [32] for the pure Marangoni problem. It is shown in Fig. 4 that by taking T_m as a reference as done by Stengel *et al.* [7], the critical Rayleigh number first increases, then reaches a maximum and finally decreases; if T_0 is used as a reference instead, a monotonic increase of Ra^c is observed. Two different vertical logarithmic scales are plotted on the right side of Fig. 4: one associated with the critical Ra curve for the case of rigid horizontal boundaries (R–R), the other one for the case of stress-free horizontal boundaries (F–F). The left vertical scale is linear and used to draw Stengel *et al.*'s curves (see Fig. 4 caption). If Ra_m denotes the Rayleigh number defined with a reference viscosity taken at T_m, then the Ra number, equation (28), used in the present work is linked to Ra_m by:

$$Ra_m = Ra\exp(-L/2). \tag{49}$$

The relationship of equation (49) allows us to recover the results of Stengel *et al.* [7] by starting from our own values for Ra^c. For completeness, the results of Fig. 1(a) are reproduced in the plane Ra_m^c–Ma_m^c of Fig. 1(b) by utilizing the mean temperature as a reference; this is accomplished by using the relationship between Ma_m and the Marangoni number of equation (32)

$$Ma_m = Ma\exp(-L/2). \tag{50}$$

The drawback of a graph like Fig. 1(b) is that the distance $\delta = \sqrt{(Ra_m^c)^2 + (Ma_m^c)^2}$ is not proportional to ΔT^c; indeed, in equation (44) the expression of δ contains in the denominator the quantity $\mu(T_m) = \mu(T_0 + \Delta T^c/2)$, which is also dependent on ΔT^c. Hence, no direct statement can be drawn from Fig. 1(b) concerning the change of stability in terms of the variation of ΔT^c.

The proportionality between δ and ΔT^c is still guaranteed for a variable thermal conductivity and a variable heat capacity, provided that the thermal diffusivity coefficient k_0 is taken at the same reference temperature T_0 as the reference viscosity. In the following, we analyse in detail the influence of each variable thermophysical property separately. Later, we shall examine the effects resulting from couplings. The surface tension is generally assumed to decrease with increasing temperature, which corresponds to a wide variety of fluids.

First suppose that only the viscosity is temperature-dependent. Stability curves with $L > 0$ correspond to a liquid layer heated from below—negative values of L would refer to a liquid film adhering to a ceiling and cooled from above with $\partial\xi/\partial T > 0$. Let ΔT_B^c be the critical temperature jump necessary to initiate convection as predicted by a Boussinesq model where the fluid viscosity is a constant $\mu_0 = \mu(T_0)$ since γ_0 is set to zero in the relationship of equation (21). Let us now take into account the temperature dependence of the viscosity and let $\mu(T_1)$ be its value at the upper boundary. When heating from below, $\mu(T_1)$ will be greater than $\mu(T_0)$ because the viscosity of a liquid is always a decreasing function of the temperature. Thus, progressing along the vertical from the bottom towards the upper surface, the medium becomes more and more viscous. On average, because a higher viscosity tends to slow down convection, onset of motion will be delayed in comparison with Boussinesq approximation where viscosity is taken to be uniform at the minimum value μ_0. Therefore the critical temperature difference ΔT^c is expected to be larger than ΔT_B^c. This conclusion is confirmed by Fig. 1(a) where

the norm δ given by equation (44) is found to be larger for $r_e > 1$ than for $r_e = 1$. In contrast, for $r_e < 1$, the layer is less stable, i.e. $|\Delta T^c| < |\Delta T_B^c|$ as shown in Fig. 1(a). In the next two paragraphs, we consider positive as well as negative values of κ_0 and χ_0 since the heat capacity and thermal conductivity of any fluid may either increase or decrease with temperature, independently of each other (see Tables 1 and 2).

For a fluid whose thermal conductivity decreases with temperature, the quantity $K(T_1)$ is larger than $K(T_0)$. On average, the whole layer is thermally more conductive than for a constant conductivity $K_0 = K(T_0)$. Since the thermal conductivity of a medium is a measure of its power to diffuse heat, the higher the conductivity, the more uniformly the thermal energy will be distributed within the medium. Thermal inhomogeneities should consequently decay faster and an increase of stability is expected. Indeed, the stability curves of Fig. 2 labelled with a parameter $r_a > 1$ are found above the reference curve ($r_a = 1$) so that the stability domain will span a larger area. Should thermal conductivity increase with the temperature, the converse reasoning holds true and a smaller stability area emerges whatever the value of $r_a < 1$.

Consider finally the case of a fluid with a variable heat capacity. Since heat capacity is a measure of the ability of the medium to retain its caloric energy, the higher the heat capacity, the longer thermal energy will dwell and accumulate within the medium. This tendency promotes thermal inhomogeneities and henceforth the occurrence of thermal convection. Consequently, by heating from below fluid layers whose heat capacity decreases with temperature, a loss of stability is observed compared to fluids with a constant heat capacity (see Fig. 3). Values of r_c larger than one actually imply a reduction of the stability region compared to the zone situated below the dashed reference curve. The same reasoning applied to the case $r_c < 1$ explains the reinforcement of stability.

The previous results are general in the sense that they are valid whatever the sign of κ_0, χ_0 or γ_0, the relative importance of the destabilizing agencies (gravity and surface-tension), the selected fluid and even the depth of the layer. Although Figs. 1–3 refer to an adiabatically insulated upper surface ($h = 0$), there is no difficulty in extending the results to non-zero Biot numbers. We have performed calculations with $h = 1000$, which corresponds to a very good heat conducting interface. The results for $h = 0$ and $h = 1000$ are presented in Fig. 5 wherein the normalized co-ordinates used by Nield [6], namely $Ra^c/\tilde{R}a^c$ and $Ma^c/\tilde{M}a^c$, are introduced. $\tilde{R}a^c$ is, in the Boussinesq approximation, the critical Rayleigh number when surface-tension effects are neglected and $\tilde{M}a^c$ is the critical Marangoni number when buoyancy is not taken into account. The values of $\tilde{R}a^c$ and $\tilde{M}a^c$ depend on the Biot number and are reported in the work of Nield [6]. Figure 5 represents the instability curves for different values of r_c. Similar curves corresponding to variable values of r_a and r_c are easily obtained. Note that by working with normalized co-ordinates, it is senseless to compare the relative variation of the distance δ (equation (45)) between families of curves associated with different Biot numbers because the angular coefficient varies with h. Indeed, in the natural co-ordinates Ra^c–Ma^c, the slope with angle θ (in degrees) of the straight line of equation (43) is fixed regardless of the values attributed to h. But, in normalized co-ordinates, one has a slope θ_N which is a function of h via the quantities $\tilde{R}a$ and $\tilde{M}a$.

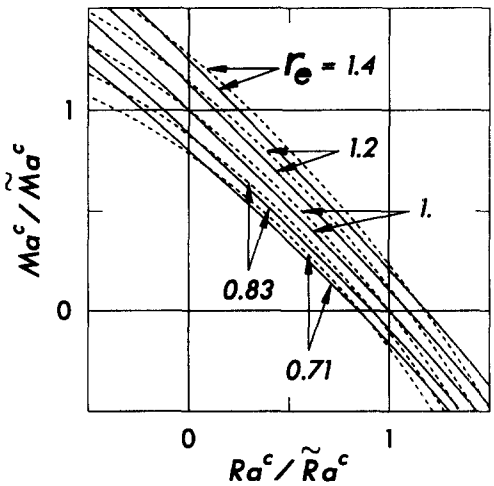

Fig. 5. Influence of a variable viscosity ($r_a = r_c = 1$) on the instability threshold in normalized co-ordinates $Ra^c/\tilde{R}a^c$–$Ma^c/\tilde{M}a^c$ for an adiabatic interface ($h = 0$, solid curves) and a heat conducting interface ($h = 1000$, dashed curves).

The above considerations are applicable to fluids whose Ra and Ma are positive. We have also extended our analysis to the cases for which Ra and Ma are negative (see Fig. 5). Recall that the area ($Ra < 0, Ma > 0$) corresponds to a situation similar to the one described with ($Ra > 0, Ma > 0$) but for a fluid whose thermal expansion coefficient has changed sign. The area ($Ra > 0, Ma < 0$) concerns fluid layers heated from above with $\alpha_0 < 0$ or liquids adhering to a cold ceiling with $\alpha_0 > 0$. When the surface tension increases with temperature, the foregoing considerations are directly applicable for the condition required to reverse the direction of heating and the direction of the gravity force. Any situation characterized by $Ra < 0$ and $Ma < 0$ is unconditionally stable.

We have also computed the critical wave number k^c in the range $1/1.3 \leqslant r_a, r_c \leqslant 1.3$ and for several Biot numbers. It is found that k^c remains practically constant. For instance, if $h = 0$, the maximum relative deviation with respect to the Boussinesq critical wave number is about 0.7% for $1/1.3 \leqslant r_a \leqslant 1.3$ and 0.2% for $1/1.3 \leqslant r_c \leqslant 1.3$. The relative differences are still smaller as h grows to infinity. For a variable heat capacity and a variable thermal conductivity, it is thus concluded that the change in k^c is negligible with respect to the values found within Boussinesq's

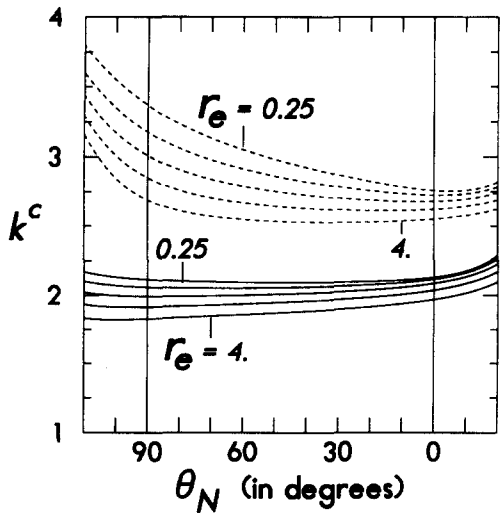

Fig. 6. Effect of a variable viscosity on the critical wave number k^c as a function of the slope θ_N (in degrees); the solid curves refer to $h = 0$ (adiabatic interface) and the dashed curves to $h = 1000$ (heat conducting interface). The values of r_e are given by 1/4, 1/2, 1, 2, 4.

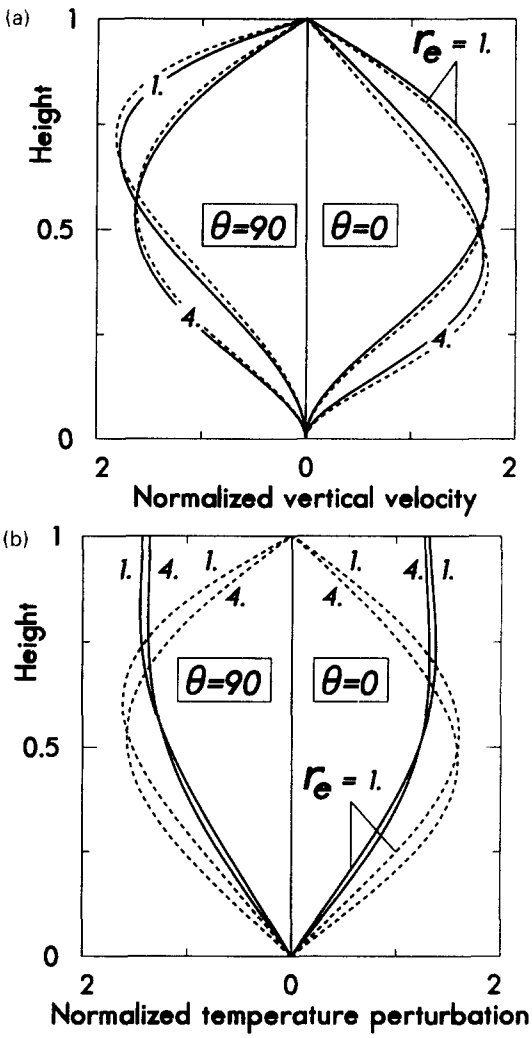

Fig. 7. (a) (b) Variation of the vertical velocity (a) and temperature disturbance (b) with the depth of the layer for a variable viscosity. Solid curves correspond to an adiabatic interface ($h = 0$), dashed curves to a good conducting interface ($h = 1000$). The right part of the figures represent the Rayleigh–Bénard instability, the left part refers to the pure Marangoni instability.

approximation. On the contrary, the deviation becomes significant when the viscosity is variable, on account of the larger values taken into practice by the parameter r_e. The critical wave number vs θ_N and the slope of the straight line passing through the origin in normalized co-ordinates is given for the two limiting cases $h = 0$ and $h = 1000$ in Fig. 6. In all cases, it is observed that k^c decreases as r_e grows. For a rigid bottom surface and a free top surface, both being perfectly heat conducting, and for $\theta_N = 0$, our result is in agreement with ref. [7], when the viscosity ratio r_e is less than 10. Comparison between the values of the critical wave number is allowed as k^c is unambiguously defined regardless of the reference viscosity.

The vertical velocity and temperature eigenfunctions are plotted in Fig. 7(a) and (b) in the limiting cases of pure Marangoni (left part of the graphs) and pure Rayleigh–Bénard instability (right part); the eigenfunctions are normalized so that their area is unitary—solid lines correspond to $h = 0$ and dashed ones to $h = 1000$. The eigenfunctions found in the Boussinesq case are not significantly modified by variable heat capacity or thermal conductivity for the parametric range considered in this work. This is the reason why only the effect of a decreasing viscosity with increasing temperature is reported. By increasing L in Fig. 7(a), one observes a strong decrease of the vertical velocity in the upper sublayer which, as explained in refs. [7] and [26] may result from the development of a viscosity stratification responsible for the formation of a stagnant lid near the cold boundary. Such an effect appears in both gravity and surface-tension driven instability problems. This is in agreement with the expected property that a larger viscosity will inhibit convective motion. Nonetheless, convective motion is more important in the vicinity of the free surface where the Marangoni effect dominates ($\theta = 90$). It is seen in Fig. 7(b) that in the cold upper part of the layer, the temperature disturbances decrease when L becomes larger.

5. COUPLING OF VARIABLE PROPERTIES

Our objective is to compare the relative effects of the various non-Boussinesq parameters on the onset of instability. The coupling of a variable heat capacity and a variable thermal conductivity is readily analysed as r_a and r_c remain small in practice. Since it is justified to use the linear reference temperature profile of equation (7), only the energy equation (38) and the thermal boundary condition, equation (33), will depend on r_a via the quantity A. First, suppose that only the thermal conductivity is temperature-dependent; after neg-

lecting the term $D\Theta$ in equation (38) and the variation of the generalized Biot number, one obtains the following stationary energy equation when A is the single non-zero parameter:

$$W = -(1+AX_3)(D^2-k^2)\Theta. \tag{51}$$

If C is the single parameter different from zero, one has instead of equation (51)

$$W = -\frac{(D^2-k^2)\Theta}{(1+CX_3)}. \tag{52}$$

Under the condition $|C| < 1$, equation (52) becomes:

$$W = -(1-CX_3)(D^2-k^2)\Theta. \tag{53}$$

From inspection of equations (51) and (53), it follows that, within the framework of the above approximations, the eigenvalues of the system are unchanged, if, instead of varying $c_p(T)$ with a rate C, $K(T)$ is varied with a rate, $-C$. This confirms the observations of Section 4, namely that temperature-dependent heat capacity and thermal conductivity play an opposite role in the onset of convection.

We now couple the remaining non-Boussinesq effects in pairs; we successively examine the effects resulting from the coupling of a variable viscosity with a variable thermal conductivity (Fig. 8(a) and (b)) and a variable heat capacity (Fig. 8(c) and (d)). For conciseness, only the limiting cases of pure surface tension (Marangoni problem) and pure buoyancy (Rayleigh–Bénard problem) instabilities are considered, the upper interface is either adiabatically insulated or perfectly heat conducting. In Fig. 8(a)–(d), the abscissa is the parameter L and the ordinate, the relative variation Δ defined by equation (45), is expressed as a percentage; curves are labelled in the function of A or C. Figure 8(a)–(d) indicates that the curves of the same family (same Biot number and same motor of instability) are quasi-parallel. This observation suggests that the various effects are to a good approximation nearly additive. This is particularly true when r_a, r_c and r_e depart little from unity. Since we know that a variable viscosity with $L > 0$ is stabilizing, it can be asserted from Fig. 8(a)–(d) that the superposition of the effects due to $L > 0$ with another stabilizing agency (i.e. $A > 0$ or $C < 0$) gives rise to an amplification of the resulting effect; the relative difference Δ is greater than the simple summation of each individual contribution, whatever the Biot number or the dominant instability mechanism, as confirmed by the diverging behaviour of the beams of curves. Similarly, the combination $L > 0$ and $A < 0$ (or $C > 0$) yields a global relative difference smaller (in algebraic value) than the result which is obtained by adding the relative difference of each separate effect. The conclusion is the opposite for $L < 0$ because the beam of curves tends to converge as L diminishes. The Biot number appears to have a significant influence when the thermal conductivity is variable (see Fig. 8(b)). It is also interesting to note that the coupling of two non-Boussinesq effects may result in a complete neutralization of these effects; this corresponds to the situations depicted in Fig. 8(a) and (b) where a Δ-curve crosses the abscissa line. In these cases, combined non-Boussinesq effects annihilate each other.

In ref. [31] we have evaluated the change in ΔT^c resulting from a variable viscosity for two liquids widely employed in Rayleigh–Marangoni experiments: silicone oil M200 and glycerol. However, as observed by Stengel *et al.* [7], the heat capacity of glycerol is not constant but varies linearly with the temperature. Other liquids like liquid metals (mercury, sodium, potassium, cadmium, etc.) are characterized by a quasi-constant heat capacity but variable viscosity and thermal conductivity. Using the experimental data of Stengel *et al.* [7] for glycerol and those of Edwards *et al.* [11] for liquid potassium, we have calculated ΔT^c as a function of the depth of the layer (see Figs. 9 and 10) and for several values of the Biot number; the labels 1, 2 and 3 correspond to $h = 0$, 10 and 1000, respectively. We have also computed ΔT^c for other liquid metals but the results are not reported here because the coupling between viscosity and thermal conductivity effects is less important than for potassium. An example where non-Boussinesq effects compensate each other is that of liquid mercury; the parameters κ_0 and γ_0 for liquid mercury have nearly the same absolute value, but are opposite in sign, while the parameter χ_0 is negligible (see Table 1). According to the discussion of Section 4, the two relevant non-Boussinesq factors have opposite effects, so that when superposed, they counterbalance each other, therefore, the difference with Boussinesq's model is hardly discernable.

The upper parts of Figs. 9 and 10 represent ΔT^c vs the depth of the layer for constant (dashed lines) and variable material properties (solid lines), respectively. On the lower part of these figures the relative difference Δ as a percentage between the non-Boussinesq and Boussinesq models (solid lines) is given. The broken lines in the lower part of Fig. 10 describe situations in which only viscosity is variable. In glycerol, the temperature T_0 at the lower boundary is taken to be equal to 25°C and in liquid potassium to be equal to 700 C. The corresponding thermophysical data for glycerol and potassium are given in Table 2. Data are collected from refs. [7, 10, 11]. The surface-tension data are taken from ref. [33] for a silicone-oil–glycerol interface and from ref. [11] for liquid potassium in contact with its vapor. The values of the coefficients α_0, κ_0, χ_0, γ_0 are obtained by fitting with a least squares method the laws given by equations (4), (8), (19), (21) with the experimental data.

In the case of glycerol, the results are practically unchanged when a variable heat capacity is introduced with respect to a model based exclusively on a variable viscosity; the differences are so small that they cannot be reproduced on a graph. Figures 9 and 10 indicate that the error which is introduced by omitting non-

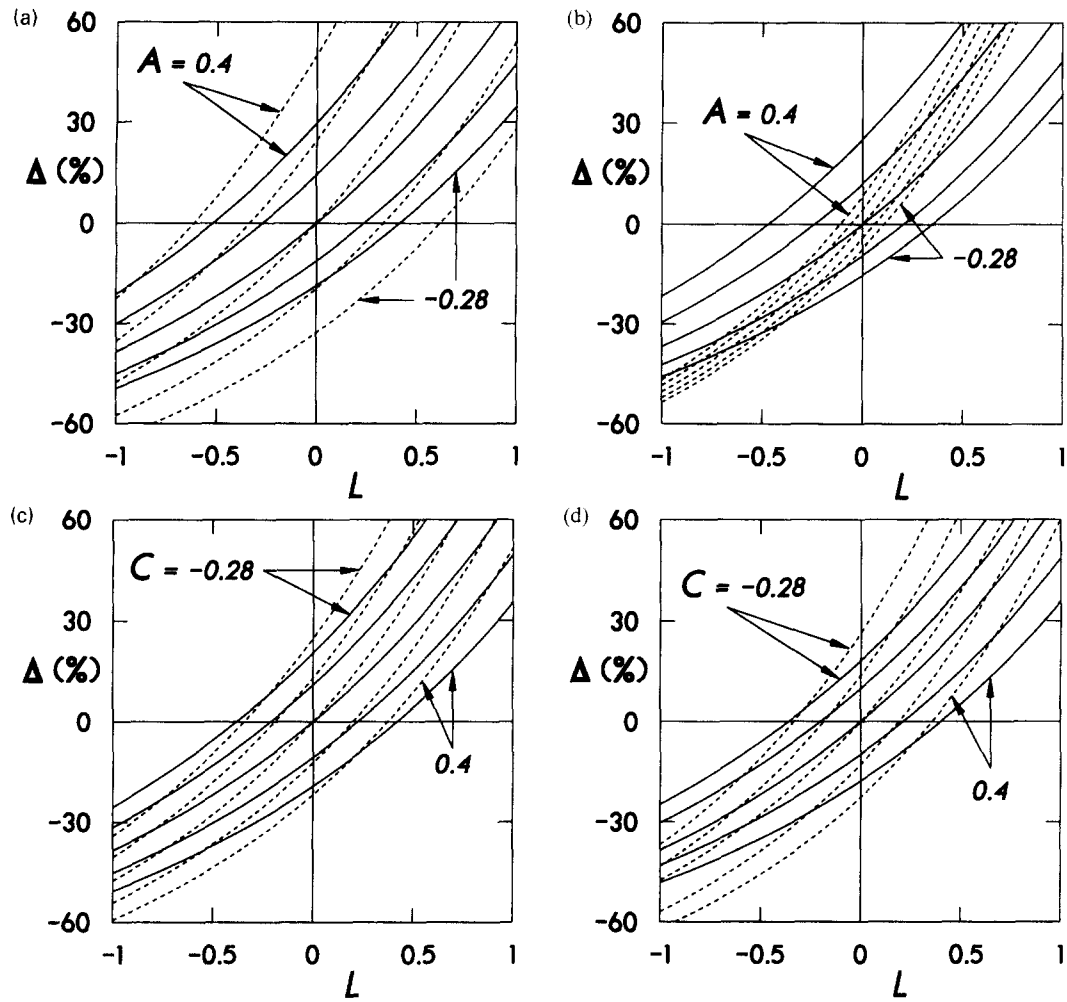

Fig. 8. (a) (b) The relative difference Δ (as a percentage) as a function of L in the case of both a variable viscosity and a variable thermal conductivity. Solid curves are for $h = 0$, dashed curves for $h = 1000$. The parameter A takes the successive values 0.4, 0.2, 0, −0.17, −0.28. (a) Pure buoyancy driven instability; (b) pure surface-tension driven instability. (c) (d) The relative difference Δ (as a percentage) as a function of L in the case of both a variable viscosity and a variable heat capacity. Solid curves are for $h = 0$, dashed curves for $h = 1000$. The parameter C takes the successive values −0.28, −0.17, 0, 0.2, 0.4. (c) Pure buoyancy-driven instability; (d) pure surface-tension driven instability.

Boussinesq effects is not small especially for very thin layers. Finally, it is observed that non-Boussinesq effects inhibit instability.

We have also checked that the inequalities $\varepsilon_1 \ll 1$ and $\varepsilon_2 \ll 1$ defining the domain of validity of the non-Boussinesq approximation are not violated even in the unfavourable case of small depths and large temperature gradients: for a glycerol layer of depth $d = 0.7$ cm and $\Delta T^c = 12°C$, one has $\varepsilon_1 = 6.10^{-3}$, $\varepsilon_2 = 6.10^{-15}$, while $L = 1.1$, $C = -0.03$; for liquid potassium with $d = 0.02$ cm and $\Delta T^c = 160°C$, it is found that $\varepsilon_1 = 0.05$, $\varepsilon_2 = 8.10^{-7}$ and $L = 0.13$, $A = 0.12$.

To our knowledge, no experimental work exists which comprehensively examines the role of non-Boussinesq effects on Bénard–Marangoni instability. An attempt to determine the critical temperature difference in an Aroclor layer may be found in Hoard *et al.*'s work [21], but these authors claim that the conditions to observe surface-tension instability are not fully respected in their experiment because of the contamination of the interface by aluminium powder added for measurement facilities. In addition, Hoard *et al.* do not report the values of the critical Marangoni number, nor the variation of surface tension with temperature, nor the value of the bottom temperature; comparison is therefore senseless. It is hoped that the present theoretical study will prompt further experimental investigations.

6. FINAL REMARKS

The aim of this work is to examine the consequences arising from the relaxation of some Boussinesq approximations, such as constant thermal conductivity, heat capacity and viscosity on the onset of convection in Rayleigh–Marangoni problem. Only infini-

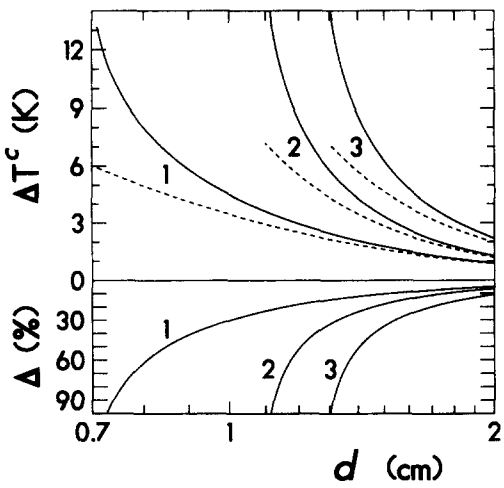

Fig. 9. Critical temperature difference ΔT^c vs the depth d of a glycerol layer (upper part of the figure) calculated within the non-Boussinesq theory (solid lines) and the Boussinesq approximation (dashed lines). The lower part of the figure gives the relative difference Δ (as a percentage) between the two results. Curves labelled 1, 2, 3 refer to Biot numbers $h = 0$, 10, 1000, respectively. The bottom temperature T_0 is fixed at 25°C.

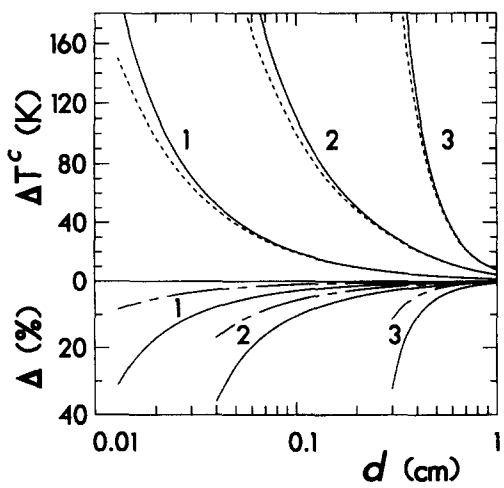

Fig. 10. Critical temperature difference ΔT^c vs the depth d of a liquid potassium layer (upper part of the figure) calculated within the non-Boussinesq theory (solid lines) and the Boussinesq approximation (dashed lines). The lower part of the figure gives the relative difference Δ (as a percentage) between the two results (solid curves). The broken lines give the percentage difference between a model wherein only the viscosity is variable and a model with constant coefficients. Curves labelled 1, 2, 3 refer to Biot numbers $h = 0$, 10, 1000, respectively. The bottom temperature T_0 is fixed at 700°C.

tesimally small disturbances are considered. Tentative physical interpretations are proposed and shed some light on the role played by the variation of the thermophysical coefficients on the onset of instability. This work is a generalization of Nield's classical analysis [6] based on Boussinesq's model.

To our knowledge, a comprehensive study including all non-Boussinesq effects in the Rayleigh–Marangoni problem has not yet been undertaken. It is true that a paper by Busse [34] was concerned with the temperature variations of the three viscometric coefficients, but Busse restricted his analysis to the Rayleigh problem. Moreover, Busse assumed that each coefficient varies linearly with the temperature and that the reference temperature profile is parabolic-like in approximation (11). Another limitation of Busse's approach is that its perturbative technique restores the linear Boussinesq equations as a first order approximation; it follows that no information can be drawn about the influence of non-Boussinesq effects on the onset of convection.

Finally, the present analysis provides a first step towards a more general non-linear description which is unavoidable in view of determining the geometrical nature of the cell pattern. In this respect, we wish to point out a recent experimental work by Nitschke and Thess [35] about a secondary instability, where it is shown that hexagonal cells are gradually replaced by square cells. Nitschke and Thess conjecture that this transition could be due to non-Boussinesq effects. Non-linear developments are presently under study and are planned to be the subject of a future paper.

Acknowledgements—The authors wish to thank the referees for their suggestions and criticisms which contributed to improve the quality of the present article. The investigation of R. Selak is supported by the 'Fonds pour la Formation à la Recherche dans l'Industrie et l'Agriculture. F.R.I.A., Belgium'. This text presents research results of the Belgian programme on Interuniversity Poles of Attraction (PAI no. 29) initiated by the Belgian State Prime Minister's Office Science Policy Programming. The scientific responsibility is assumed by the authors.

REFERENCES

1. Chandrasekhar, S., *Hydrodynamic and Hydromagnetic Stability*, Chaps 1 and 2. Oxford University Press, London, 1961.
2. Mihaljan, J. M., A rigorous exposition of the Boussinesq approximations applicable to a thin layer of fluid. *Astrophysics Journal*, 1962, **136,** 1126–1133.
3. Gray, D. D. and Giorgini, A., The validity of the Boussinesq approximation for liquids and gases. *International Journal of Heat and Mass Transfer*, 1976, **19,** 545–551.
4. Normand, C., Pomeau, Y. and Velarde, M. G., Convective instability: a physicist's approach. *Review of Modern Physics*, 1977, **49,** 581–624.
5. Pérez-Cordon, R. and Velarde, M. G., On the (non-linear) foundations of Boussinesq approximation applicable to a thin layer of fluid. *Journal de Physique*, 1975, **36,** 591–601.
6. Nield, D. A., Surface-tension and buoyancy effects in cellular convection. *Journal of Fluid Mechanics*, 1964, **19,** 341–352.
7. Stengel, K. C., Oliver, D. S. and Booker, J. R., Onset of convection in a variable-viscosity fluid. *Journal of Fluid Mechanics*, 1982, **120,** 411–431.
8. Jenkins, D. R., Rolls vs squares in thermal convection of fluids with temperature-dependent viscosity. *Journal of Fluid Mechanics*, 1986, **178,** 491–506.
9. Chen Y. M. and Pearlstein, A. J., Onset of convection in variable viscosity fluids: assessment of approximate viscosity-temperature relations. *Physics of Fluids*, 1988, **31,** 1380–1385.

10. Weast, R. C., *Handbook of Chemistry and Physics*, 68th edn. C.R.C. Press, Boca Raton, FL, 1987–1988.
11. Edwards, D. K., Denny, V. E. and Mills, A. F., *Transfer Processes: an Introduction to Diffusion, Convection and Radiation*, 2nd edn, Appendix B. McGraw-Hill, New York, 1978.
12. Pearson, J. R., On convection cells induced by surface-tension. *Journal of Fluid Mechanics*, 1958, **4,** 489–500.
13. Busse, F. H., Non-linear properties of thermal convection. *Reports on Progress in Physics*, 1978, **41,** 1929–1967.
14. Collatz, L., *The Numerical Treatment of Differential Equations*, 3rd edn, Chap. 3. Springer-Verlag, New York, 1966.
15. Coddington, E. A. and Levinson, N., *Theory of Ordinary Differential Equations*, Chap. 3. McGraw-Hill, New York, 1955.
16. Stakgold, I., *Green's Functions and Boundary Value Problems*, Chap. 3. Wiley, New York, 1979.
17. Vidal, A. and Acrivos, A., Nature of the neutral state in surface-tension driven convection. *Physics of Fluids*, 1966, **9,** 615.
18. Takashima, M., Nature of the neutral state in convective instability induced by surface tension and buoyancy. *Journal of the Physical Society of Japan*, 1970, **28,** 810.
19. Rossby, H. T., A study of Bénard convection with and without rotation. *Journal of Fluid Mechanics*, 1969, **36,** 309–335.
20. Pampaloni, E., Pérez-Garcia, C., Albavetti, L. and Ciliberto, S., Transition from hexagons to rolls in convection in fluids under non-Boussinesq conditions. *Journal of Fluid Mechanics*, 1992, **234,** 393–416.
21. Hoard, C. Q., Roberton, C. R. and Acrivos, A., Experiments on the cellular structure in Bénard convection. *International Journal of Heat and Mass Transfer*, 1970, **13,** 849–856.
22. Cerisier, P., Jamond, C., Pantaloni, J. and Pérez-Garcia, C., Stability of roll and hexagonal patterns in Bénard–Marangoni convection. *Physics of Fluids*, 1987, **30,** 954–959.
23. Davaille, A. and Jaupart, C., Transient high-Rayleigh-number thermal convection with large viscosity variation. *Journal of Fluid Mechanics*, 1993, **253,** 141–166.
24. Booker, J. R., Thermal convection with strongly temperature-dependent viscosity. *Journal of Fluid Mechanics*, 1976, **76,** 741–754.
25. Richter, F. M., Experiments on the stability of convection rolls in fluids whose viscosity depends on temperature. *Journal of Fluid Mechanics*, 1978, **89,** 553–560.
26. Richter, F. M., Nataf, H.-C., and Daly, S. F., Heat transfer and horizontally averaged temperature of convection with large viscosity variations. *Journal of Fluid Mechanics*, 1983, **129,** 173–192.
27. White, D. B., The planforms and onset of convection with a temperature-dependent viscosity. *Journal of Fluid Mechanics*, 1988, **191,** 247–286.
28. Carey, V. P. and Mollendorf, J. C., Variable viscosity effects in several natural convection flows. *International Journal of Heat and Mass Transfer*, 1980, **23,** 95–109.
29. Busse, F. H. and Frick, H., Square-pattern convection in fluids with strongly temperature-dependent viscosity. *Journal of Fluid Mechanics*, 1985, **150,** 451–465.
30. Bottaro, A., Metzener, P. and Matalon, M., Onset and two-dimensional patterns of convection with strongly temperature-dependent viscosity. *Physics of Fluids*, 1992, **4,** 655–663.
31. Selak, R. and Lebon, G., Bénard–Marangoni thermoconvective instability in presence of a temperature-dependent viscosity. *Journal de Physique*, II, 1993, **3,** 1185–1199.
32. Slavtchev, S. and Ouzounov, V., Stationary Marangoni instability in a liquid layer with temperature-dependent viscosity, in microgravity. *Microgravity Quarterly*, 1994, **4,** 33–38.
33. Cardin, Ph., Nataf, H.-C. and Dewost, Ph., Thermal coupling in layered convection: evidence for an interface viscosity control from mechanical experiments and marginal stability analysis. *Journal de Physique*, II, 1991, **1,** 599–622.
34. Busse, F. H., The stability of finite amplitude cellular convection and its relation to an extremum principle. *Journal of Fluid Mechanics*, 1967, **30,** 625–649.
35. Nitschke, K. and Thess, A., Secondary instability in surface-tension-driven Bénard convection. *Physical Review*, 1995, E**52,** 5772–5775.